Sensors and Materials, Vol. 13, No. 8 (2001) 487–497
MYU Tokyo

S & M 0464

Technique for Sensing Potential Distributions on Insulating Materials with Surface Discharge Using Pockels Device

Akiko Kumada[1], Masakuni Chiba[2] and Kunihiko Hidaka[2]

[1]Tokyo Electric Power Company, 4-1 Egasakicho, Tsurumi-ku, Yokohama, Japan
[2]Department of Electrical Engineering, Graduate School of Engineering, The University of Tokyo

(Received January 31, 2001; accepted September 2, 2001)

Key words: Pockels, surface discharge, potential, nanosecond, distribution, measurement

A new method has been developed for measuring the transient potential distribution of surface discharge. The measuring system consists of an Ar ion laser, a beam expander, a streak camera, a charge coupled device (CCD) camera, and a sensing device with a $Bi_4Ge_3O_{12}$ (BGO) Pockels crystal. Two types of sensors have been developed and the features and properties of these sensors have been checked experimentally. One type can be applied to the high-accuracy measurement required for clarifying the propagation mechanism of surface discharge. The other is expected to be applicable for measuring surface discharge phenomena under varying conditions.

1. Introduction

Surface discharge on a dielectric material has a great influence on the insulating performance of electrical apparatus and electronic devices. Information on the potential and the field profile along the surface discharge is required to quantitatively discuss and clarify the propagation mechanism.[1,2]

Sensing techniques using Pockels crystals have been applied to the measurement of space charge in electrical discharge.[3,4] The techniques are expected to make it possible to directly measure the distribution of the potential and the electric field of a surface streamer. We propose a new system for measuring the transient potential distribution of surface discharge without any disturbance to the electric field distribution.[4–7] As the sensing device of this measuring system, a disk $Bi_4Ge_3O_{12}$ (BGO) crystal with a diameter of 50 mm

is used. With this sensing device, the potential distribution of surface discharge can be measured directly without any potential divider.

In this paper, another sensing device is explained which includes a capacitive divider in its structure. The features and properties of each sensing device are evaluated and discussed.

2. Measurement System

2.1 *Principle and experimental setup*

Figure 1 shows the schematic diagram of the measurement system. The linearly polarized light beam emitted from an Ar ion laser (514.5 nm in wavelength, 50 mW in power, 1.5 mm ϕ in laser diameter) is expanded to a width of 50 mm with a cylindrical beam expander, squeezed to a thickness of 0.2 mm with a cylindrical lens, and then sent into a BGO (relative permittivity $\varepsilon_r = 16$) crystal with a diameter of 50 mm. As shown in Fig. 2, surface discharge occurs and propagates directly on the surface of the BGO.

The BGO shows the Pockels effect and the polarization of the light transmitted through it is changed. One side of the BGO is grounded and the reverse side has a dielectric-mirror coating. The laser beam is reflected back by the dielectric mirror on the crystal, and only the x-axis component of it is detected through a polarized beam splitter by a streak camera system. The detected light intensity I_{out} is given by

$$I_{out} = \frac{1}{2} I_{in} \{1 - \cos(k \cdot V_{BGO})\}, \tag{1}$$

where I_{in} is the input light intensity, k is a constant and V_{BGO} is the potential difference applied to the BGO.

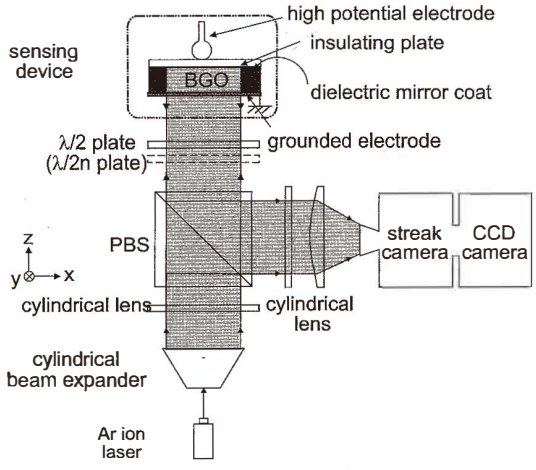

Fig.1. Schematic diagram.

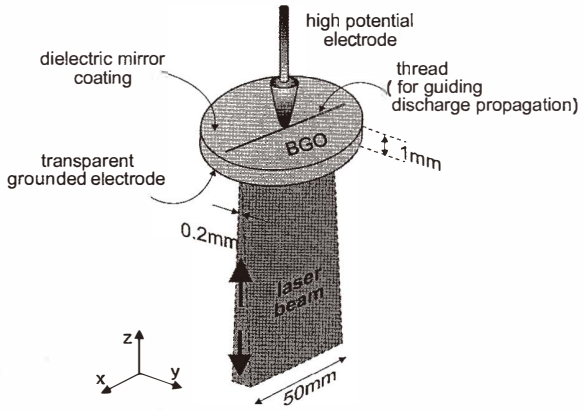

Fig. 2. Sensing device.

The change over time in the beam intensity distribution is observed with a streak camera, which is connected to a charge coupled device (CCD) camera (512×512 pixels) to digitize the output light intensity. To calibrate an exact potential value on the BGO, a plate electrode is attached on the insulating plate and the light intensities are measured at all points on the measuring surface of the plate while the voltage applied to the plate electrode is changed. From this data, an equation showing the relationship between the output light intensity and the potential on the BGO is derived for all 512 points along the measured linear path of 50 mm.

With this system, the potential profile on the surface of the BGO along a linear path with a maximum length of 50 mm can be measured quantitatively and consecutively without causing any field disturbance. Considering the specification of the streak camera system such as the streaking speed, the number of pixels of the CCD camera and the resolution of the CCD camera tubes, the minimum resolution of this system reaches 20 μm in the space domain and 2–3 ns in the time domain.

Equation (1) shows that the detected light intensity changes as a cosine function of the potential difference applied to the BGO. This relation also shows that there is a limited range in the measured potential difference for holding a single-value relationship between the detected light intensity and the potential difference. This limit is defined as the half wavelength voltage V_π. The value V_π for this BGO is 14.5 kV.

2.2 *Transient response characteristics*

The transient response characteristic of the measurement system is examined by applying an impulse voltage of 75 ns in risetime to the plane electrode that is set on the BGO. The output waveform of the measurement system at the center of the BGO is shown in Fig. 3 compared with the applied impulse voltage. The system responds well to the applied voltage.

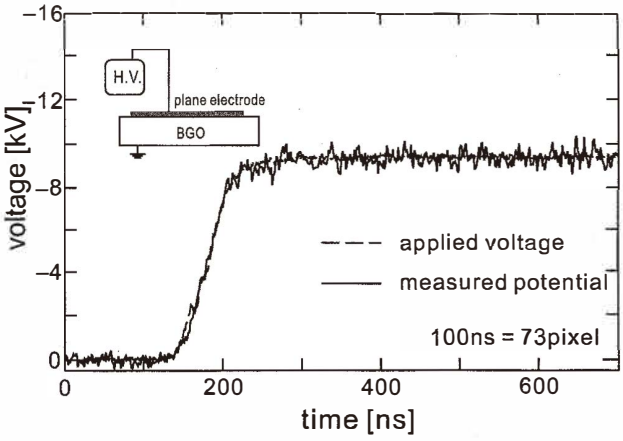

Fig. 3. Transient response.

The fluctuation of the signal due to various kinds of noise occurring in the laser and the CCD camera is observed on the profiles of the measured potential. The magnitude of this fluctuation depends on the intensity of the detected light, which corresponds to the potential on the BGO. The relationship between the standard deviation σ of the fluctuation and the instantaneous measured potential V is estimated based on the experimental data. An example is shown in Fig. 4. In this figure, the value of σ increases with V. In the case of $V = -5$ kV and -10 kV, σ is 0.17 kV (3.4%) and 0.46 kV (4.6%), respectively.

2.3 *Potential distribution near a rod electrode*

The potential distribution near a rod electrode was measured to check the measurement accuracy. The 5 mm ϕ rod electrode is set parallel to the y-axis on the BGO surface in an insulating oil pool to suppress the occurrence of surface discharge.

Figure 5 shows the potential distribution obtained at the moment when a potential of –6.0 kV is applied to the rod electrode. The error bar is added to the potential profile using the relationship shown in Fig. 4. The theoretical potential is also shown in Fig. 5. It is obtained on the basis of numerical computation using the charge simulation method. The experimental result agrees well with the theoretical one.

2.4 *Potential distribution along a surface discharge*

Figure 6 shows an example of the change in potential distribution with the propagation of a surface discharge on the BGO. The 4 mm ϕ spherical electrode is exactly at the position of $x = 0$ mm, and a positive step voltage (risetime = 90 ns, V_{peak} = 6.75 kV) is applied. With the propagation of surface discharge, the high-potential region expands. The potential gradient inside the streamer is 8 ~ 10 kV/cm. This experimental data is indispensable to quantitatively discuss and clarify the propagation mechanism.

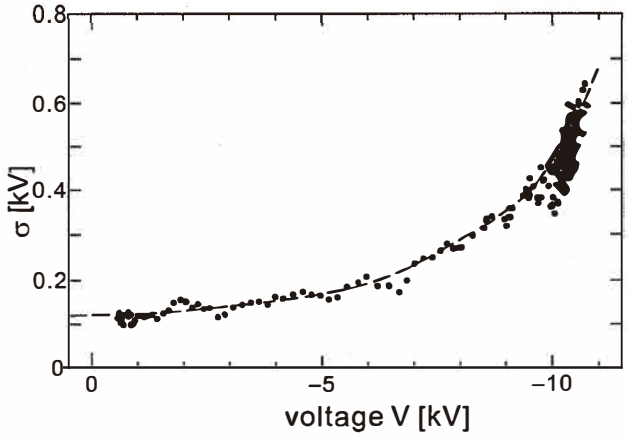

Fig. 4. Standard deviation of measured potential.

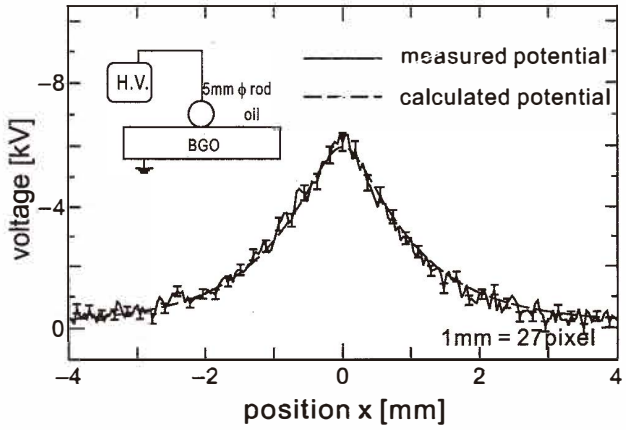

Fig. 5. Potential distribution near a rod electrode.

3. Capacitive Dividing Sensor

The surface discharge phenomena is influenced by many experimental factors such as the condition of the insulating plate, the waveform of the applied voltage, the composition of the environmental gas and so on. The sensing device mentioned in the previous section can be applied to the surface discharge phenomena only under restricted conditions. To measure the surface discharge under various conditions, a capacitive dividing sensor has been developed. Its properties and features are evaluated in this section.

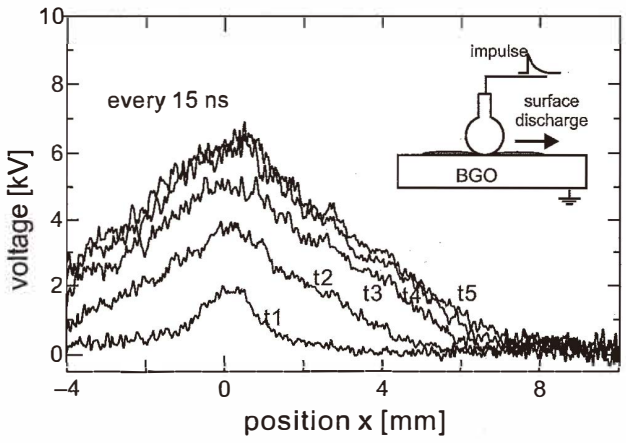

Fig. 6. Potential distribution along a positive streamer.

3.1 *Structure of sensor*

Figure 7 shows the "prototype sensor" which was made on a trial basis. A BGO crystal, whose dimensions are 4×3×50 mm, is set in a 4-mm-thick acrylic plate. Capacitive divided potential is applied to the BGO.

This prototype sensor was proven to have difficulty in measuring with high accuracy.[2] Due to thermal contraction of the acrylic plate surrounding the BGO, the optical adjustment angle of the BGO changes with time. The total optical loss of the measurement system varies during the measurement period required for calibration. The influence of this variation is so large that it is difficult to derive a reasonable experimental equation for calibration.

Figure 8 shows the "capacitive dividing sensor." This sensor has an improved mold for the crystal. A BGO crystal, which has dimensions of 4×3×50 mm and which is surrounded by the same thick BGO crystals, is covered with an insulating plate such as glass or acrylic.

3.2 *Calibration*

A capacitive divided potential is applied to the BGO. The electric field calculation is needed to estimate the potential profile on the insulating plate from the measured potential profile on the BGO.

The coaxial model and the boundary conditions for the electric field calculation with the charge simulation method are shown in Fig. 9. The number of unknown parameters (substitute charges and the true surface charges on the insulating plate) equals the number of equations representing boundary conditions. The electric field and potential distribution on the insulating plate can be determined analytically. In practice, the solution of this inverse problem is so sensitive to the measurement errors that it is hardly obtained.

Inversely, if we define the potential profile on the insulating plate, we can easily calculate the potential profile on the BGO. Using a repetitive process where we assume a

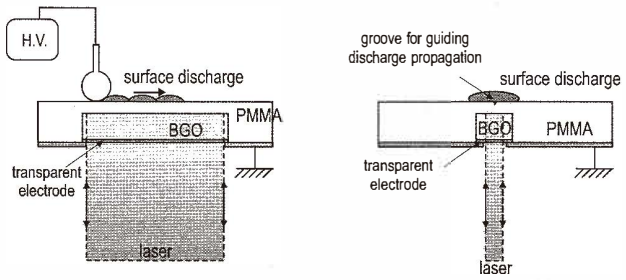

Fig. 7. Prototype sensor.

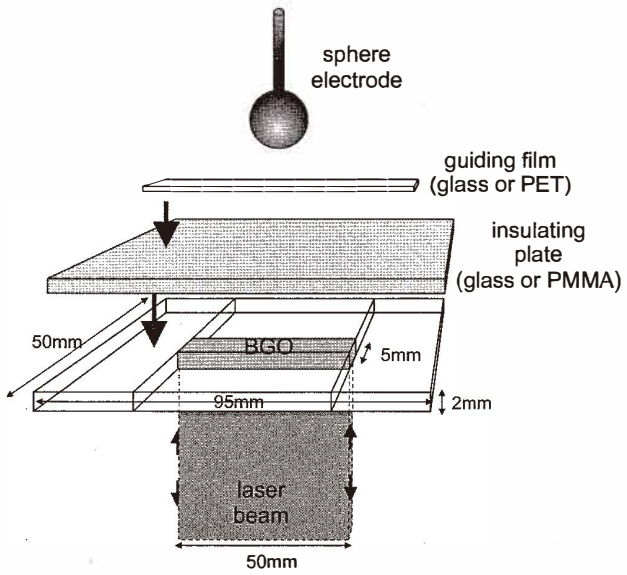

Fig. 8. Capacitive dividing potential sensor.

potential profile on the insulating plate, calculate the potential profile for the BGO and compare it to the experimental data, we can approach a reasonably accurate potential profile on the insulating plate.

3. 3 *Experimental results*

3.3.1 *Potential distribution near a rod electrode*

To examine the calibration method mentioned in section 3.2, the potential distribution near an 8 mm ϕ rod electrode was measured. An AC voltage (50 Hz) is applied to the rod electrode which is set on a 1-mm-thick glass insulating plate. Figure 10 shows the potential

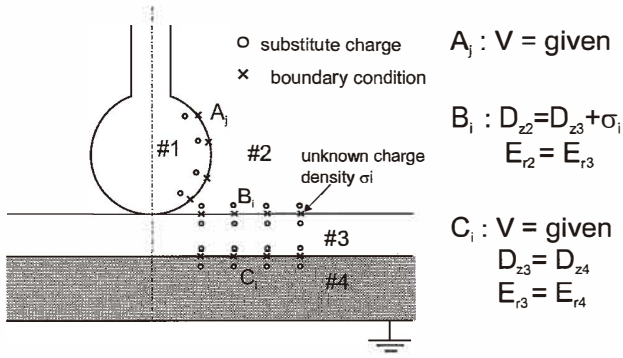

Fig. 9. Coaxial model for electric field calculation with charge simulation method.

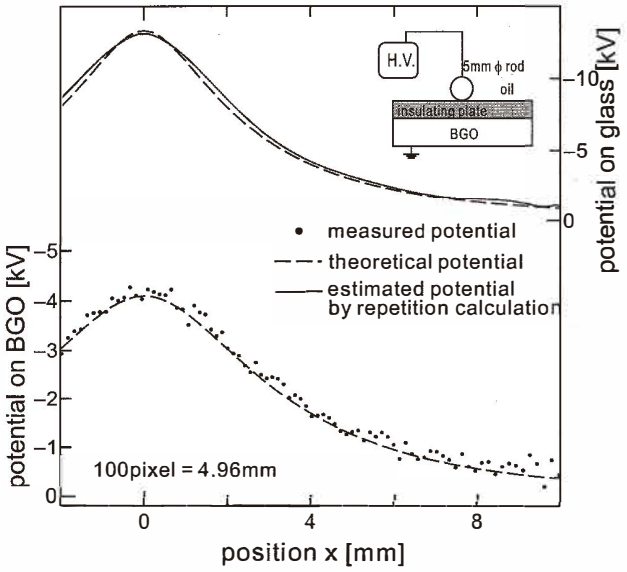

Fig. 10. Potential distribution near a rod electrode.

distributions on the insulating plate and the BGO at the moment a potential of –13.2 kV is applied to the electrode. The estimated potential on the insulating plate agrees well with the theoretical potential obtained on the basis of numerical computation.

However, in the case that potential distribution forms a very sharp profile, the estimated profile tends to become gentle. To improve the accuracy, it is preferable to use this sensor in combination with a potential difference probe as shown in Fig. 11.[4]

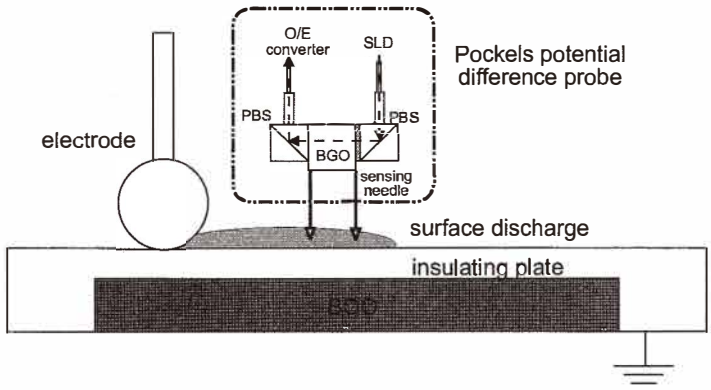

Fig. 11. Combination with potential difference probe.

3.3.2 *Frequency response characteristics*

When a voltage in the low frequency range is applied to the insulating plate, a resistive divided voltage is applied to the BGO. In the case where a 1-mm-thick PMMA (polymethyl methacrylate, $\varepsilon_r = 2.3$) is used as the insulating plate, the lower frequency limit of the "capacitive divided sensor" is calculated to reach 10^{-1} Hz as shown in Fig. 12.

To check this lower frequency limit experimentally, a DC voltage test was performed as follows: The insulating plate (PMMA, 1 mm thick) is charged instantaneously by a negative surface discharge. The charge of surface discharge remains on the insulating plate as a residual charge. The change in the potential distribution on the BGO surface is measured for a long term.

As shown in Fig. 13, the potential distribution on BGO changes gradually and forms a "flat shape" within 1 s after the insulating plate is charged by a surface discharge. The equivalent circuit of the "capacitive dividing sensor" as shown in Fig. 14 explains this phenomenon. The dielectric mirror coating decreases the conductive resistance on the BGO surface. The conductive current flows and the potential distribution on BGO changes to a certain flat value.

It is possible to measure the potential distribution near the rod electrode when a 50 Hz AC voltage is applied as shown in Fig. 10. The lower frequency limit of this capacitive divided sensor is estimated at 10 ~ 50 Hz. To broaden frequency bandwidth, improvements in the dielectric mirror are needed.

4. Conclusions

As the sensing device of the potential distribution measurement system, two sensors which structurally exclude/include a potential divider are developed. The features of these sensors are listed in a comparative table in Table 1.

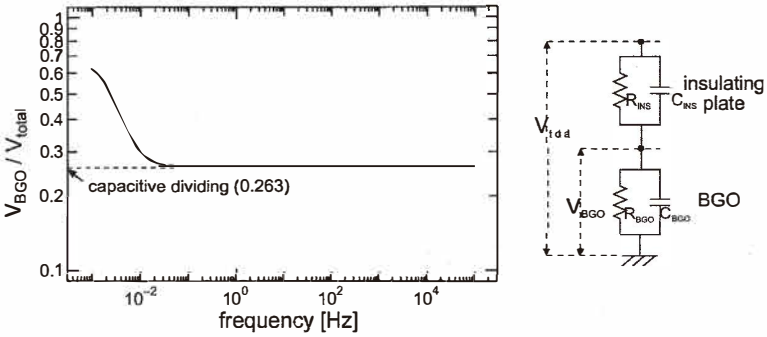

Fig. 12. Frequency response characteristics.

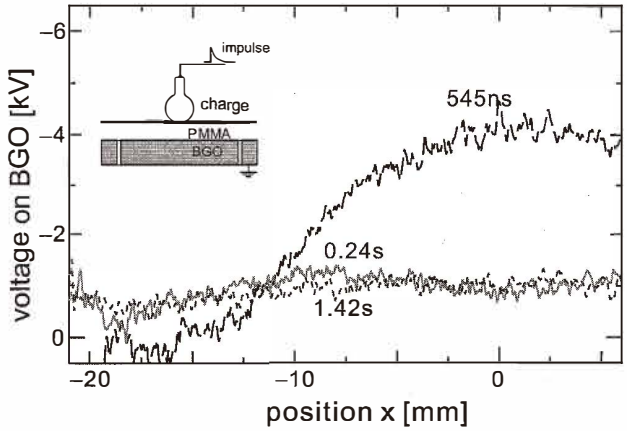

Fig. 13. Reformation of potential distribution.

The former sensor has advantages in accuracy and frequency bandwidth (DC~GHz). This sensor, however, requires restricted experimental conditions such as the voltage limitation based on V_π, the material and thickness of insulating plate.

On the other hand, the latter sensor is useful to measure surface discharge phenomena under various conditions. The lower frequency limit of this sensor is expected to reach 10^{-1} Hz. In reality, due to the conductivity of the dielectric mirror coating, the lower frequency limit is higher at 10~50 Hz. By incorporating an electric field calculation, it is possible to estimate the potential profile on the insulating plate. To enhance accuracy, the combined measurement with a potential difference sensor is better.

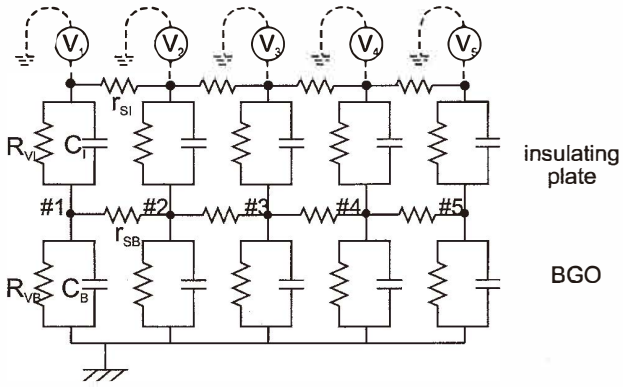

Fig. 14. Equivalent circuit of capacitive dividing sensor.

Table 1
Features of sensors.

	Direct measuring sensor	Capacitive dividing sensor
Measurement range	0 ~ 14 kV	Variable
Target & applications	Under restricted conditions	Under various conditions
Accuracy	High-accuracy	Needs electric field calculation
Frequency responsibility	DC ~	10^{-1} Hz~

References

1 I. Gallimberti: Journal of Applied Physics **5** (1972) 2179.
2 S. Larigaldie: Journal of Applied Physics **76** (1994) 3724.
3 K. Hidaka: IEEE Electrical Insulation Magazine **12** (1996) 17.
4 T. Kawasaki, T. Terashima, S. Suzuki and T. Takada *et al.*: Journal of Applied Physics **76** (1994) 3724.
5 A. Kumada, M. Chiba and K. Hidaka: Journal of Applied Physics **84** (1998) 3059.
6 A. Kumada, M. Chiba and K. Hidaka: T. IEE Japan **118**-A (1998) 723.
7 A. Kumada, M. Chiba and K. Hidaka: T. IEE Japan **120**-A (2000) 204.